

Delay Margin for Predictive PI Control System¹⁾

ZHU Hong-Dong SHAO Hui-He

(Department of Automation, Shanghai Jiaotong University, Shanghai 200030)

(E-mail: hongdongzhu@sjtu.edu.cn)

Abstract The variation of plant dead-time deeply affects the stability of the predictive PI control system. It is important for designing and applying the PPI controller to calculate the delay margin. A criterion of stability for the PPI system and the quantitative relationship among the delay margin, the time constant of the closed-loop system, and the dead-time of the model are given. A graphic algorithm to compute the delay margin is also developed. The phenomenon that there exist more than one stability delay zones is discussed. The algorithm is shown to be precise by some simulations.

Key words Predictive PI, stability analysis, stability delay margin

1 Introduction

Due to its simple structure, more than 95% of the control loops are of the PID type in process control. Most loops are actual PI control^[1]. In addition, the process control engineers accumulate abundant knowledge of maintaining and applying the PID controllers. However, when controlling the process with delay using the PID controller, the phase of the control loop is increased because of the existence of delay. Then, the phase margin is decreased. In order to obtain enough stability margins, the gain cross-over frequency must be decreased, which will reduce the bandwidth and performance of the closed-loop system.

An additional dead-time compensator in controller will highly improve the performance of the delay system. The Smith predictor and internal model control are always two adopted methods^[2~3]. Since both of them are model-based control methods and need a precise model of the plant, the closed-loop stability is sensitive to the modeling error, especially the modeling error of dead-time. A little modeling error of dead-time may destabilize the system. In addition, more tuning parameters are needed in these kinds of controllers than those of the PID controller. All above factors restrict the application of the controllers with dead-time compensator. On the other hand, owing to the fact that the dead-time compensator will highly improve the performance of the closed-loop system, many researchers are devoted to tuning controller parameters and analyzing the stability of the closed-loop system.

Hagglund proposed a tuning method for the Smith predictive control, which was called predictor PI (PPI) control^[4]. The PPI controller had only three adjustable parameters: process gain, time constant of the closed-loop system, and the dead-time. The first order plus dead-time model was used to tune the PPI controller. The PPI control system was tuned to the first order plus dead-time process, in which the dead-time and the time constant of the closed-loop system were chosen as the dead-time and α times of the time constant of the model, respectively. The PPI controller is successfully applied to actual process control. In [5], a low-pass filter was introduced to the PPI control systems, which improved the robustness of the closed-loop systems. In [6], a new robust tuning method was proposed. The first order plus dead-time model and the relative modeling error were obtained by the moment identification method. When tuning the parameters of the PPI controller, a specified variation of dead-time was considered. This tuning method is conservative to the estimation of the variation of the plant dead-time.

PPI controller is a special case of Smith predictor control strategy. Therefore, the PPI system also inherits the shortcoming of the Smith predictive control, *i.e.*, it is sensitive to the dead-time variation. So it is of great theoretical and practical significance for guiding design and application of the PPI controller to research the effect of the variation of the plant dead-time.

In this paper, the stability analysis of the PPI system in frequency domain is proposed. A new stability criterion for the PPI system is given. The relationship among the delay margin, dead-time

1) Supported by "863" High-Tech Research and Development Program of P. R. China (2001-AA413130)

Received December 16, 2003; in revised form August 1, 2004

of the plant, and the time constant of the closed-loop system are obtained. A graphic algorithm to compute the delay margin is also given, which enables the designer to do better in comprehending and applying the PPI controller.

The paper is arranged as follows: at first, the short review of the PPI controller is given in Section 2. Section 3 gives a new stability theorem for the PPI system and its proof. In Section 4, the quantitative relationship among the delay margin, the time constant of the closed-loop system, and the dead-time of plant are given. In addition, a graphic method of computing delay margin is proposed, whose accuracy is also shown by some simulation examples. The phenomenon that more than one delay stability zones exist in the PPI system is indicated and discussed. Finally, the paper ends with some concluding remarks.

2 PPI controller

The control scheme of the PPI control system is shown in Fig. 1, where $P(s)$ is the plant, $P_m(s) = P_0(s)e^{-\tau_0 s}$ is the model of the plant, $P_0(s) = \frac{K_0}{T_0 s + 1}$ is the delay-free part of the model, and $C_0(s)$ is a PI controller. Therefore, the $C(s)$ that is composed of $C_0(s)$, $P_0(s)$, and $P_m(s)$ is called PPI controller. The tuning rule for the PPI controller is to tune the transfer function of the closed-loop system to the first order plus dead-time process:

$$G_{yr}(s) = \frac{Y(s)}{R(s)} = \frac{1}{\lambda s + 1} e^{-\tau_0 s} \quad (1)$$

where λ is the time constant of the closed-loop system. Then, the PPI controller has the following form:

$$C(s) = \frac{T_0 s + 1}{K_p(\lambda s + 1 - e^{-\tau_0 s})} \quad (2)$$

In order to reduce the number of the adjustable parameters, Haggund suggested that the time constant of closed-loop system should be α times of the time constant of the controlled plant, *i.e.*, $\lambda = \alpha T_0$. In this case, $C_0(s)$ has the following form:

$$C_0(s) = K_p \left(1 + \frac{1}{T_i s} \right) \quad (3)$$

where $K_p = \alpha/(\alpha K_0)$, $T_i = T_0$. If α is larger than 1, the step response of the closed-loop system is slower than that of the plant, while if α is smaller than 1, the step response of closed-loop system is faster than that of the plant. Haggund suggested that α should be 1. The aim of the control method is to reduce the tuning parameters by constructing a relationship of time constant between the closed-loop system and the controlled plant. Since the PPI controller is a Smith predictor with the special tuning rule, the stability of the closed-loop system is affected by the variation of the dead-time of the plant.

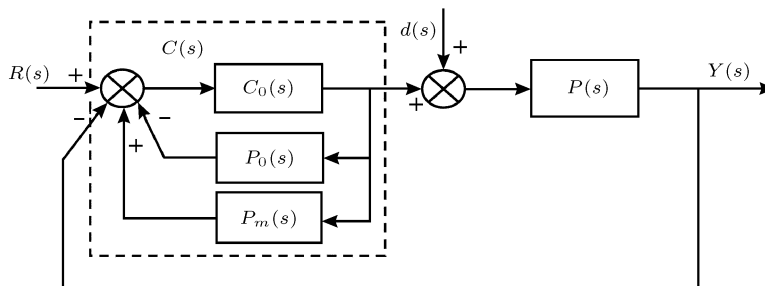


Fig. 1 The PPI control system

3 Stability analysis of the PPI control system

The stability analysis of the PPI control system was not proposed in [4]. Robust stability of the PPI system was discussed in some literature when unstructured uncertainty existed in the controlled plant. No method for computing the delay margin was given in time domain. In this section, we

analyze the stability of the PPI system in frequency domain utilizing Nyquist stability criterion. When the delay-free part of the model is matched with that of the plant, the loop transfer function of the PPI control system is

$$L(s) = \frac{e^{-\tau s}}{\lambda s + 1 - e^{-\tau_0 s}} \quad (4)$$

where λ , τ_0 , and τ are the time constant of the closed-loop system, the dead-time of the model, and the dead-time of the controlled plant, respectively. Substituting $s = j\omega$ and Euler formula into (4) yields

$$L(j\omega) = \frac{\cos(\tau\omega) - j \sin(\tau\omega)}{1 - \cos(\tau_0\omega) + j(\lambda\omega + \sin(\tau_0\omega))} \quad (5)$$

Simplify it and we obtain

$$\begin{aligned} \operatorname{Re}(L(j\omega)) &= \frac{\cos(\tau\omega) - \cos(\tau\omega)\cos(\tau_0\omega) - \sin(\tau\omega)\sin(\tau_0\omega) - \lambda\omega\sin(\tau\omega)}{2 - 2\cos(\tau_0\omega) + 2\lambda\omega\sin(\tau_0\omega) + \lambda^2\omega^2} \\ \operatorname{Im}(L(j\omega)) &= -\frac{\sin(\tau\omega) + \cos(\tau\omega)\sin(\tau_0\omega) - \sin(\tau\omega)\cos(\tau_0\omega) + \lambda\omega\cos(\tau\omega)}{2 - 2\cos(\tau_0\omega) + 2\lambda\omega\sin(\tau_0\omega) + \lambda^2\omega^2} \end{aligned} \quad (6)$$

where $\operatorname{Re}(\cdot)$ and $\operatorname{Im}(\cdot)$ are the functions that get the real part and imaginary part of a complex number, respectively. Let $x = \operatorname{Re}(L(j\omega))$, $y = \operatorname{Im}(L(j\omega))$, and

$$\begin{aligned} a(\omega, \tau, \tau_0, \lambda) &= \frac{-\cos(\tau\omega)\cos(\tau_0\omega) - \sin(\tau\omega)\sin(\tau_0\omega)}{2 - 2\cos(\tau_0\omega) + 2\lambda\omega\sin(\tau_0\omega) + \lambda^2\omega^2} \\ b(\omega, \tau, \tau_0, \lambda) &= \frac{-\cos(\tau\omega)\sin(\tau_0\omega) + \sin(\tau\omega)\cos(\tau_0\omega)}{2 - 2\cos(\tau_0\omega) + 2\lambda\omega\sin(\tau_0\omega) + \lambda^2\omega^2} \\ r(\omega, \tau, \tau_0, \lambda) &= \frac{\sqrt{1 + \lambda^2\omega^2}}{2 - 2\cos(\tau_0\omega) + 2\lambda\omega\sin(\tau_0\omega) + \lambda^2\omega^2} \end{aligned} \quad (7)$$

Then, the relationship among the x , y , a , and b is

$$(x - a)^2 + (y - b)^2 = r^2 \quad (8)$$

It can be found out obviously from (8) that the Nyquist curve of the PPI loop transfer function is a cluster of circles in the complex plane, whose centers and radius of the cluster circles are (a, b) and r , respectively. However, (a, b) and r are all related to ω , τ_0 , τ , λ . When τ_0 equals τ , (7) can be rewritten as

$$\begin{aligned} a(\omega, \tau_0, \lambda) &= \frac{-1}{2 - 2\cos(\tau_0\omega) + 2\lambda\omega\sin(\tau_0\omega) + \lambda^2\omega^2} \\ b(\omega, \tau_0, \lambda) &= 0 \\ r(\omega, \tau_0, \lambda) &= \frac{\sqrt{1 + \lambda^2\omega^2}}{2 - 2\cos(\tau_0\omega) + 2\lambda\omega\sin(\tau_0\omega) + \lambda^2\omega^2} \end{aligned} \quad (9)$$

It is concluded from (9) that the centers of the cluster circles are on the real axis in complex plane and changed with the variation of ω . A theorem will be proved firstly before the stability criterion for the PPI system is given.

Theorem 1. For all λ and τ_0 , the unity feedback system with the loop transfer function $L_1(s) = \frac{1}{\lambda s + 1 - e^{-\tau_0 s}}$ is always stable and the transfer function $L_1(s)$ has no pole on the right half complex plane.

Proof. Substituting $s = j\omega$ and Euler formula into $L_1(s)$ yields

$$L_1(j\omega) = \frac{1}{1 - \cos(\tau_0\omega) + j(\lambda\omega + \sin(\tau_0\omega))} \quad (10)$$

It can be rewritten as

$$L_1(j\omega) = \frac{(1 - \cos(\tau_0\omega)) - j(\lambda\omega + \sin(\tau_0\omega))}{(1 - \cos(\tau_0\omega))^2 + (\lambda\omega + \sin(\tau_0\omega))^2} \quad (11)$$

It can be seen that $\text{Re}(L_1(j\omega))$ is not smaller than 0 if ω varies from 0 to $+\infty$. In other words, for all λ and τ_0 the Nyquist curve will be on the first and fourth quadrant of the complex plane and the phase angle is not larger than -90 degrees. On this condition, the unity feedback system must be stable. Since the Nyquist curve of $L_1(j\omega)$ does not encircle the $(-1, 0)$ and the Nyquist criterion is necessary and sufficient condition, no pole of $L_1(s)$ is on the right half complex plane. \square

Before the stability criterion for PPI control system is proposed, we define the distance from $(-1, 0)$ point to the circle center of the Nyquist curve of $L(s)$ as

$$\varphi(\omega, \tau, \tau_0, \lambda) = \sqrt{\left(-1 + \frac{\cos(\tau\omega)\cos(\tau_0\omega) + \sin(\tau\omega)\sin(\tau_0\omega)}{2 - 2\cos(\tau_0\omega) + 2\lambda\omega\sin(\tau_0\omega) + \lambda^2\omega^2}\right)^2 + \left(\frac{\cos(\tau\omega)\sin(\tau_0\omega) - \sin(\tau\omega)\cos(\tau_0\omega)}{2 - 2\cos(\tau_0\omega) + 2\lambda\omega\sin(\tau_0\omega) + \lambda^2\omega^2}\right)^2}$$

Theorem 2. Given τ_0 , τ and λ , if

$$\frac{r(\omega, \tau, \tau_0, \lambda)}{\varphi(\omega, \tau, \tau_0, \lambda)} < 1 \quad (12)$$

for all ω , where $0 \leq \omega < +\infty$, then the PPI system is stable.

Proof. For all given τ_0 , τ and λ , if ω varies from 0 to $+\infty$ and $\frac{r(\omega, \tau, \tau_0, \lambda)}{\varphi(\omega, \tau, \tau_0, \lambda)} < 1$ holds, the Nyquist curve of $L(s)$ does not encircle the $(-1, 0)$ point, *i.e.*, the number of counterclockwise encirclements of the $(-1, 0)$ point is equal to zero. On the other hand, the distribution of the poles of $L(s)$ is the same as that of $L_1(s)$. It can be concluded that $L(s)$ has no pole on the right half complex plane. According to Nyquist stability criterion, the PPI system is stable. \square

4 Delay margin of the PPI control system

Definition. Delay margin of the PPI control system is the variation of the plant dead-time round the dead-time of the model in which the closed-loop system is stable when no model mismatch exists in the delay-free part of the plant. Although the stability of the PPI control system can be analyzed by Theorem 2, it is difficult to obtain an analytical solution of the delay margin of the PPI system. Thus, we propose a numeric method of computing the delay margin of the PPI system according to the Nyquist curve of the PPI system. At first, the characteristic of the Nyquist curve of $L_0(s)$ is illustrated when the model is precise, *i.e.*, $\tau = \tau_0$.

1) Asymptotic characteristic. For the real part and imaginary part of $L_0(j\omega)$, we have

$$\begin{cases} \lim_{\omega \rightarrow 0^+} \text{Re}(L_0(j\omega)) = -\frac{\tau_0^2 + 2\lambda\tau_0}{2(\tau_0 + \lambda)^2} \\ \lim_{\omega \rightarrow 0^+} \text{Im}(L_0(j\omega)) = -\infty \end{cases} \quad (13)$$

The initial position and the asymptotic line of the Nyquist curve of $L_0(s)$ are $(-\frac{\tau_0^2 + 2\lambda\tau_0}{2(\tau_0 + \lambda)^2}, -\infty)$ and $x = -\frac{\tau_0^2 + 2\lambda\tau_0}{2(\tau_0 + \lambda)^2}$, respectively.

2) Rotation characteristic. If ω is large enough, the Nyquist curve of $L_0(s)$ behaves towards rotation characteristic. It is composed of a cluster of circles with the center and radius of the circle being $(\frac{-1}{2 - 2\cos(\tau_0\omega) + 2\lambda\omega\sin(\tau_0\omega) + \lambda^2\omega^2}, 0)$ and $\frac{\sqrt{1 + \lambda^2\omega^2}}{2 - 2\cos(\tau_0\omega) + 2\lambda\omega\sin(\tau_0\omega) + \lambda^2\omega^2}$, respectively.

3) Convergence characteristic. When ω tends to ∞ , the Nyquist curve of $L_0(j\omega)$ tends to the origin because

$$\begin{aligned} \lim_{\omega \rightarrow \infty} a(\omega) &= \lim_{\omega \rightarrow \infty} \frac{-1}{2 - 2\cos(\tau_0\omega) + 2\lambda\omega\sin(\tau_0\omega) + \lambda^2\omega^2} = 0 \\ \lim_{\omega \rightarrow \infty} r(\omega) &= \lim_{\omega \rightarrow \infty} \frac{\sqrt{1 + \lambda^2\omega^2}}{2 - 2\cos(\tau_0\omega) + 2\lambda\omega\sin(\tau_0\omega) + \lambda^2\omega^2} = 0 \end{aligned} \quad (14)$$

In other words, the radius and the center of the cluster of the Nyquist circles tend to zero.

In order to illustrate the characteristic of the Nyquist curve of $L_0(s)$, a Nyquist curve is shown in Fig. 2 when $\tau_0 = \tau = 10$, $\lambda = 1.2$, where the real line and the dashed line are the Nyquist curve and the unit circle, respectively. There are five points whose magnitudes are one. The five points are called gain-crossover points. The corresponding frequencies are called gain-crossover frequencies.

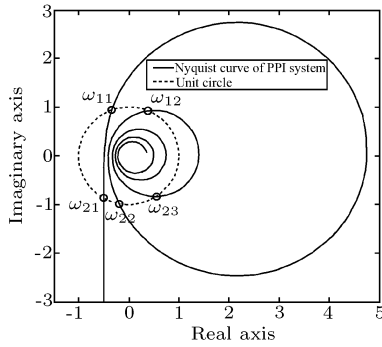


Fig. 2 The Nyquist curve of $L_0(s)$ when model is precise and $\tau_0 = \tau = 10$, $\lambda = 1.2$

Here, the proposed method of computing delay margin is demonstrated through Fig. 2. The five points in Fig. 2 are divided into two groups. The first group has two points ω_{11} and ω_{12} , which are at the first quadrant and the second quadrant of the complex plane. The corresponding phase angles of the two points are Φ_{11} and Φ_{12} , respectively. The other group has three points ω_{21} , ω_{22} , and ω_{23} , which are at the third quadrant and the fourth quadrant of complex plane. The corresponding phase angles of these points are Φ_{21} , Φ_{22} , and Φ_{23} , respectively.

Suppose that the variation of the dead-time of the controlled plant is $\Delta\tau$, *i.e.*, $\tau = \tau_0 + \Delta\tau$. The loop transfer function of the PPI control system is changed to

$$L'(s) = \frac{e^{-\tau_0 s}}{\lambda s + 1 - e^{-\tau_0 s}} e^{-\Delta\tau s} = L_0(s)e^{-\Delta\tau s} \quad (15)$$

This is equivalent to serialing a delay part whose dead-time is $\Delta\tau$ to the transfer function $L_0(s)$ in the case of no model mismatch. The magnitude and the phase angle of $e^{-\Delta\tau s}$ are 1 and $-\Delta\tau\omega$, respectively. According to the operation rule of the complex number, when the dead-time of the plant varies to $\tau_0 + \Delta\tau$, the magnitude of $L'(j\omega)$ is the same as that of $L_0(j\omega)$ and the difference of phase angles between $L'(j\omega)$ and $L(j\omega)$ is $-\Delta\tau\omega$. If $\Delta\tau$ is positive, the Nyquist curve of $L'(j\omega)$ can be obtained by rotating Nyquist curve of $L_0(j\omega)$ by $\Delta\tau\omega$ clockwise. On the other hand, if $\Delta\tau$ is negative, the Nyquist curve of $L'(j\omega)$ can be obtained by rotating Nyquist curve of $L_0(j\omega)$ by $\Delta\tau\omega$ counterclockwise. It should be pointed out that the rotation degree of the point of Nyquist curve is relevant to the frequency of the point. Observing the five points in Fig. 2, when $\Delta\tau$ decreases gradually from zero, one point of the first group will rotate firstly to $(-1, 0)$ point because the angle to $(-1, 0)$ point is small in the counterclockwise direction, which is called lower boundary gain crossover point (LBGCP). Thus, the system is critically stable and the step response in time domain is continuously oscillatory. We call the now dead-time of the plant as the low boundary of delay margin (LBDM), *i.e.*, $\tau_{low} = \tau_0 + \Delta\tau$ and call the frequency of LBGCP lower boundary gain cross over frequency (LBGCF). If $\Delta\tau$ keeps on decreasing, the point of intersection of the real axis and the Nyquist curve is on the left part of $(-1, 0)$ point. The closed-loop system is unstable. On the other hand, when $\Delta\tau$ increases gradually from zero, one point of the second group will rotate firstly to $(-1, 0)$ point because the angle to $(-1, 0)$ point is small in the clockwise direction, which is called upper boundary gain crossover point (UBGCP). Thus, the system is critically stable and the step response in time domain is continuous oscillatory. We call the now dead-time of plant as the upper boundary of delay margin (UBDM), *i.e.*, $\tau_{up} = \tau_0 + \Delta\tau$ and call the frequency of UBGCP upper boundary gain cross over frequency (UBGCF). As above mentioned, the LBDM and UBDM can be calculated by the following formulae:

$$\tau_{low} = \tau_0 - \min_{i=1,2,\dots,m} \left(\frac{\pi - \Phi_{1i}}{\omega_{1i}} \right) \quad (16)$$

$$\tau_{up} = \tau_0 + \min_{i=1,2,\dots,n} \left(\frac{\pi + \Phi_{2i}}{\omega_{2i}} \right) \quad (17)$$

where m and n are the numbers of intersection points in the upper part and lower part of complex plane, respectively.

Through extensive simulating, some conclusions about the distribution of the intersection points of the Nyquist curve of $L_0(s)$ and unit circle can be drawn.

1) The number of the intersection points is only relative to τ_0/λ . When $\tau_0/\lambda < 2.9843$, the number of the intersection points is one. The intersection point is on the third quadrant of the complex plane. In other words, the magnitude of the Nyquist curve will not be larger than one after the Nyquist curve enters into the unit circle.

2) When $\tau_0/\lambda > 2.9843$, the number of the intersection points is larger than one, *i.e.*, the Nyquist curve of $L_0(s)$ crosses over the unit circle as shown in Fig. 2. The larger τ_0/λ is, the larger the number of the intersection points is. If τ_0/λ of two loop transfer functions that have different parameters τ_0 and λ are the same, the numbers of intersection points of the two systems are also the same.

3) If two systems have the same τ_0/λ and different λ , the gain cross-over frequencies of the same gain cross-over points of the two systems are in inverse proportion to λ of the two systems, *i.e.*,

$$\frac{\omega_1}{\omega_2} = \frac{\lambda_2}{\lambda_1} \quad (18)$$

According to the above conclusions, all gain cross-over points can be obtained by the numeric method. Based on the gain cross-over frequencies of these points and (16) and (17), the delay margin of a PPI system can be calculated. It is known from the third conclusion that only the upper cross-over frequency ω_{up} and lower gain cross-over frequency ω_{low} need to be calculated with different τ_0/λ when $\lambda = 1$. ω_{up} and ω_{low} for any τ_0/λ can be calculated by (18). Then, the delay margin of the PPI system can be obtained. ω_{up} and ω_{low} are calculated and shown in Fig. 3 when $\lambda = 1$ and τ_0/λ varies from 0.001 to 20 with step length 0.001. Since τ_0/λ of the practical process is generally in this range, the results in Fig. 3 can fit the most actual PPI systems. The procedure of calculating delay margin of the PPI system with any τ_0 and λ is summarized as follows.

- 1) Find ω_{up} and ω_{low} according to τ_0/λ of the given PPI system and Fig. 3.
- 2) Substitute ω_{up} , ω_{low} , and λ to (18) and obtain ω'_{up} and ω'_{low} .
- 3) Substitute ω'_{up} and ω'_{low} to (5) and calculate the phase angles of the two points. Using (16) and (17), the delay margin can be calculated.

The delay margins of the PPI system in which $\lambda = 1$ and τ_0/λ varies from 0.001 to 20 are shown in Fig. 4. Some remarkable notes about Fig. 3 and Fig. 4 are made as follows.

1) That ω_{low} equals zero in Fig. 3 means only one intersection point of the Nyquist curve and unit circle. The lower boundary of delay margin is zero in this case.

2) ω_{up} is smaller than ω_{low} at some τ_0/λ . Two factors that make a gain cross-over point be UBGCP or LBGCP are its frequency and phase angle. When the UBGCP and LBGCP are in different circles of Nyquist curve, this phenomenon will occur.

3) There may be many stability delay zones on the PPI system. According to Theorem 1, the PPI system is always stable for all τ_0 and λ when the dead-time of the plant is zero. However, the lower boundary of delay margin of the PPI system in which $\tau_0/\lambda > 2.9843$ is not zero. The reason is that the delay margin of the PPI system is a stability delay range around the dead-time of the process model. If we can solve the stability criterion proposed in Section 2, all stability delay zones can be obtained. It should be pointed out that the other delay stability ranges are small. Although the closed-loop system is stable when the dead-time is in the other delay stability range, the step response of the PPI system is oscillatory or slow.

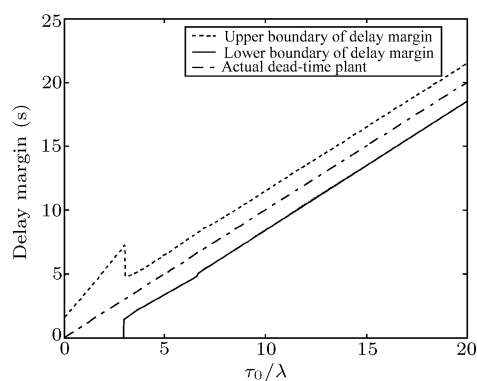
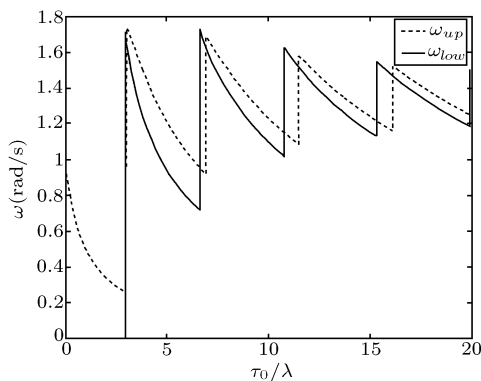


Fig. 3 UBGCF and LBGCF of the PPI system

Fig. 4 The delay margin of the PPI system when $\lambda = 1$

Some simulation results will be given to show the precision of the proposed algorithm of computing the delay margin. Suppose that the dead-time of the plant is 20. The delay margin, LBGCF, and

UBGCF are shown in Table 1 when the closed-loop time constant is set to 2, 5, 10, 15, 20, 25, and 30. The step responses in time domain are shown in Fig. 5 when the time constant of the closed-loop system is 5 and dead-time of the plant is set to be 27.4315 and 12.5102, respectively. It can be seen in Fig. 5 that the PPI system is continuously oscillatory when the dead-time of the plant is set to be the upper boundary and lower boundary of the delay margin. It is evident that the method of computing the delay margin is precise.

Table 1 Delay margin, UBGCF, and LBGCF in different time constants, where $\tau_0 = 20$

λ	2	5	10	15	20	25	30	35
ω_{up}	0.6165	0.2904	0.0342	0.0291	0.0253	0.0224	0.0202	0.0183
ω_{low}	0.5500	0.2365	0	0	0	0	0	0
τ_{up}	22.9746	27.4315	52.5442	59.6463	66.9692	74.4062	81.8969	89.4826
τ_{low}	16.9528	12.5102	0	0	0	0	0	0

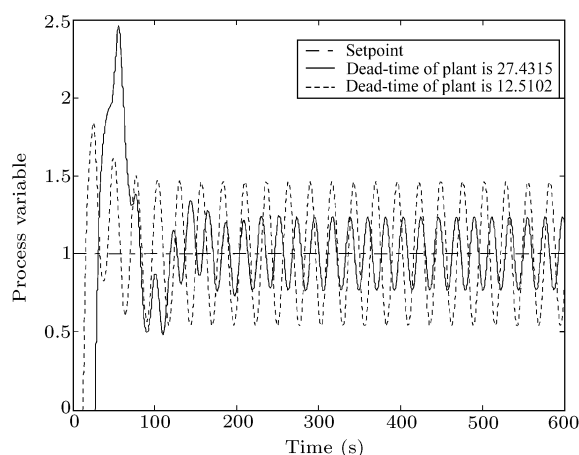


Fig. 5 Step response of the PPI system when the dead-time of plant varies to 27.4315 and 12.5102 where $\lambda = 5, \tau_0 = 20$

5 Conclusion

A stability criterion for the PPI system is proposed. The quantitative relationship among the delay margin, the time constant of closed-loop PPI system, and the model dead-time are given when the delay-free part of model is matched by that of the plant. We also develop a graphic algorithm of computing the stability delay margin and discuss the phenomenon that there exist more than one stability delay zones. The algorithm is shown to be precise by simulations.

References

- 1 Aström K J, Haggund T. PID Controllers: Theory, Design, and Tuning. North Carolina: Instrument Society of America, 1995
- 2 Smith O J M. Closed control of loops with dead time. *Chemical Engineering Progress*, 1957, **53**(5): 217~219
- 3 Morari M, Zafriou E. Robust Process Control. New Jersey: Prentice-Hall, Englewood Cliffs, 1989
- 4 Haggund T. An industrial dead-time compensating PI controller. *Control Engineering Practice*, 1996, **4**(6): 749~756
- 5 Normey-Rico J E, Bordons C, Camacho E F. Improving the robustness of dead-time compensating PI controllers. *Control Engineering Practice*, 1997, **5**(6): 801~810
- 6 Ari Ingimudarson, Tore Haggund. Robust tuning procedures of dead-time compensating controllers. *Control Engineering Practice*, 2001, **9**(11): 1195~1208

ZHU Hong-Dong Received his master degree from Henan University of Science and Technology in 2001. He is currently a Ph. D. candidate in the Department of Automation at Shanghai Jiaotong University. His research interests include auto-tuning of controller for the delay system, nonlinear control, and bioreactor control.

SHAO Hui-He Professor in the Department of Automation at Shanghai Jiaotong University. His research interests include MPC, advance process control, identification, soft sensor, and bioreactor control.